4th World Congress on Gearing
and Power Transmission

Paris, France ---- March, 1999

Comparison of Experimental and Analytical Tooth Bending Stress of Aerospace Spiral Bevel Gears

Robert F. Handschuh

Army Research Laboratory
NASA Lewis Research Center
Cleveland, Ohio, 44135
U.S.A.

George D. Bibel
University of North Dakota
Department of Mechanical Engineering
Grand Forks, North Dakota, 58202-8359
U.S.A.

Comparaison de la tension de courbure des dents analytique et expérimentale des engrenages coniques en vrille aérospatiaux

Robert F. Handschuh
Army Research Laboratory
NASA Lewis Research Center
Cleveland, Ohio, 44135
Etats-Unis

George D. Bibel
University of North Dakota
Department of Mechanical Engineering
Grand Forks, North Dakota 58202–8359
Etats-Unis

Une étude analytique et expérimentale fut réalisée pour déterminer la tension de courbure dans les engrenages coniques en vrille aérospatiaux. Un modèle limité d'éléments de l'engrenage conique en vrille utilisé lors des tests fut analysé. Les tests furent exécutés par le centre d'essai Lewis des engrenages coniques en vrille de la NASA. Plusieurs dents sur le pignon conique en vrille furent instrumentées avec des jauges de tension et des tests furent réalisés à des vitesses variant de statique à 14 400 tr/min, à une puissance de 540 kW (720 c.v.). Les effets des changements de vitesse et de charge sur la tension de courbure furent mesurés. Les résultats expérimentaux ont été comparés à ceux de l'analyse du modèle limité d'éléments en trois dimensions.

INTRODUCTION

Spiral bevel gears are currently used in all main rotor drive systems for rotorcraft produced in the United States. Applications such as these require spiral bevel gears to turn the corner from the horizontal engine to the vertical rotor. These gears are typically required to operate at extremely high rotational speeds and carry high power levels. With these difficult operating conditions, successful operation is paramount to aircraft safety and reliability.

The analysis and testing of spiral bevel gears has been very sparse in the open literature in comparison to that which exists for parallel axis gears. This is due to the complex gear geometry and specialized test equipment necessary to test these components. Over the last fifteen years analytical work has been directed at trying to understand and develop the theoretical basis for predicting the operational behavior of this type of gear (Refs. 1-7). From the basic gear geometry treatment of describing the manufacturing kinematics via a differential geometry approach, these methods have been extended to build full three dimensional models of the pinion and gear based on the machine tool settings (Refs. [8-11]). This work has led to predictions of thermal and structural effects in spiral bevel gears (Refs. [12-17]).

At the same time, experimental work has been underway at a limited number of institutions to validate some of the predictions made by various numerical techniques. Some of this work has been conducted by various helicopter manufacturers to develop a data base of successful operation (Refs. [18-21]). The work that has been published in the open literature from aerospace applications has served as the upper bound on successful spiral bevel gear applications.

The objective of the work presented in this paper is to investigate the effects of rotational speed and torque on bending stress and to compare these results to an analytical model. A three-dimensional contact analysis using finite element analysis will be compared to results attained via strain gages. Experiments were conducted from static (slow-roll) to high rotational speeds (14400 RPM) at various levels of load (up to 541 kW (725 hp)).

I. ANALYTICAL MODEL DEVELOPMENT

The spiral bevel gear type used in the analysis and experiments that will be described in this report are the face-milled, tapered-tooth type. The kinematics necessary for model development used in this study is based on the work of Litvin (Ref. [3,4]). References [1-4] are the foundation for the techniques described in References [9,14,15,17].

A model was developed using the basic design variables and machine tool settings that are given in Table 1. A seven-tooth model, three pinion teeth and four gear teeth, was generated using a one-tooth sector of each gear mesh member and then duplicating the geometry to attain the finite element model. A commercially available geometry program was used to accomplish this task (Ref. [22]). The model used for this study is shown in Figure 1. The seven-tooth model of the pinion and gear have (three pinion teeth and four gear teeth) 8793 elements (eight node isoparametric elements used) and 11262 nodes that resulted in a total of 33748 degrees of freedom. A finite element analysis code (Ref. [23]) was used to conduct the analysis. This finite element code can simulate three-dimensional contact without the use of gap elements. The results used in this study were generated in References [15,17].

The model was statically loaded by fixing the pinion as shown in Figure 1 and applying a low level of torque to the gear member. This causes the gear teeth to rotate into the pinion teeth and make contact. The load was increased in the model until it equaled the experimental torque. An example of the output from the analysis for the pinion teeth is shown in Figure 2. In the work contained in Reference [15], this analysis procedure was repeated for different orientations of the model pinion and gear. The pinion was rotated a total of 36 degrees (seven increments) to simulate the loading sequence on the pinion. The data plotted (and discussed later) was found by extrapolation of Gauss point calculated values to the surface.

The finite element program used to conduct the analysis has a self-contained contact algorithm. With this feature a complex model, such as that used in this study, requires a large amount of computer processing time. This is due to a non-penetration constraints between the pinion and gear elements. Therefore the stiffness matrix needs to be reformulated at each load level during the solution sequence.

II. TEST FACILITY AND TEST HARDWARE

The test facility used for this study was the Spiral Bevel Gear Test Rig at NASA Lewis Research Center. A cross-sectional view of the facility is shown in Figure 3. The facility operates in a closed-loop, torque regenerative fashion. Two sets of spiral bevel gears are tested simultaneously in the facility. The gear mesh on the right side (slave side) of the facility operates in a speed increaser mode with the gear driving the pinion. The left side (test side) of the facility operates in a speed reducer mode where the pinion drives the output gear. The instrumented pinion used in these results was installed in the test side of the facility.

The facility is driven by v-belts from a 74.6 kW (100 hp) DC motor. A split coupling and thrust piston supplied the load transmitted in the loop (see Figure 3). The drive motor only needs to supply the power losses of the test rig. A torquemeter that is part of the power path measures the gear torque and gear shaft speed. A more complete description of the facility can be found in Reference [24].

The pinion member of the spiral bevel gear mesh was instrumented with strain gages. A photograph of the pinion used in the experiments is shown in Figure 4. A total of five strain gages were installed on the pinion. Three successive teeth were instrumented with strain gages located approximately at one-half the face width. Also the middle tooth had gages located as shown in Figure 5. The strain gages used in this study had an active gage length of 0.38 mm (0.015 in.).

III. DATA ACQUISITION

All strain gage data was recorded using a FM tape recorder. The stain gage data was transferred from the rotating pinion shaft using a slip ring. Data was taken statically and dynamically. Strain gage data was taken in the "static" or slow-roll through mesh by rotating the slave gear pinion shaft manually while the load was applied. Several revolutions of the pinion shaft were made while the load was held constant and the strain gage signals were recorded. The data was downloaded from the tape recorder to an analog to digital processor contained in a personal computer. Data taken at slow-roll conditions were not averaged.

Strain gage data was taken in the dynamic mode after the test facility had sustained a given set point of rotational speed and applied torque before any measurements were made. Dynamic data was recorded on tape for approximately one minute at a given condition. The recorded data was downloaded to a personal computer via an analog to digital processor. The dynamic data was time synchronous average. All dynamic data presented in this report was averaged with one hundred data records (except at pinion shaft speeds below 6000 RPM where fifty data records were averaged) based on one rotation of the gear shaft. Because of the exact 3:1 ratio of the test rig, three revolutions of the pinion were recorded for one rotation of the gear member.

All strain gage data was converted from voltage to engineering units assuming a uniaxial stress field was applied in the direction that the strain gages were oriented (Ref. [25]). Offsets from the tape recorder, along with the shunt values from internal wheatstone bridge resistors were used to make the calculations. The dynamic data was downloaded from the tape recorder to the analog to digital personal computer board at 250 kHz (except at low rotational speeds as mentioned above). Five analog to digital channels at this rate equates to a 50 kHz sample rate for each channel. Calibration signals were also recorded prior to testing to adjust for tape recorder output

errors. Finally the data was shifted to have the unloaded average stress equal to zero during the time when the instrumented teeth were not carrying load.

IV. COMPARISON OF ANALYTICAL AND EXPERIMENTAL RESULTS

A - Analytical Results. The analytical model described earlier was loaded statically via the three-dimensional contact capability of the finite element code of Ref [23]. The model was rotated to simulate moving through the meshing process. This was accomplished by rotating the grid point locations by the appropriate amounts based on the gear ratio. This was done for 36 degrees of pinion rotation in 6 degree increments. A contact tolerance (a separation distance at which the surfaces are considered to be in contact) of 0.0051 mm (0.0002 in.) was used in the analysis. Several locations on two successive teeth in the fillet / root region were monitored during the "meshing" process. The stress found at the various increments of pinion rotation are given in Table 2 for locations at the toe, mid-face and heel locations. The peak maximum principal stress found was 0.958 GPa (139 ksi) at the mid-face tooth fillet location. These stress values were found for the output torque on the gear equaling 1073 N*m (9500 in*lb).

B - Experimental Results. Testing was conducted in the facility described earlier at various speeds and loads. The results will be described from the slow roll through mesh to the highest speed and load conditions. Data will be described using the rotational speed of the pinion and the torque measured on the gear shaft as shown in Figure 3.

The slow-roll through mesh data was taken at gear shaft torque of 520 to 1185 N*m (4600 to 10490 in*lb). This represents 50 to 110% of the nominal operating torque of the test facility for this gear mesh. An example of the slow roll data is given in Figure 6. The data shown in Figure 6 was for a single meshing cycle. The slow-roll data was downloaded from the tape recorder at 25 samples per second. Since the data was not downloaded at a high sampling rate some of the peak stresses may have been missed. However, all the slow-roll data appeared similar to that shown in Figure 6. The stress was highest at the mid-face positions with tooth "B" having the highest stress. Also the maximum value of the heel gage stress (gage #2) was always less than that of the mid-face gages and greater than the toe gage (gage #4).

An example of the dynamic data taken is shown in Figure 7. The data shown is for the three mid-face width gages. The symbols on Figure 7 indicate the frequency of the data sampling. The data for one gear revolution is shown in Figure 8 for the same conditions (three pinion revolutions). In Figure 8 the data shows the gage on tooth "B" was consistently higher than the stress measured at the other two teeth. The difference between these three mid-face gages is believed to be due to their placement in the fillet / root region. Since the strain gage and the radius of the fillet/root region are of comparable size, placement of the gage will affect the result. Placement of a strain gage closer to the root would be more sensitive to the compressive stress due to the load being applied to the tooth prior to meshing (tooth A) than that where the gage is further up the fillet toward the tooth tip (tooth C). Therefore gage placement is very critical with respect to the maximum stress found in the experiments as the measurements were made in a high-stress gradient region.

Next, as shown in Figure 9, are the results from all three strain gages on the middle tooth (tooth "B") as shown in Figure 4. The data shown in Figure 9 was taken at 14400 RPM and 1073 N*m (9500 in*lb) of gear shaft torque. Note that the results are the same with respect to relative magnitudes between the regions of the fillet as was found in the slow-roll test as shown in Figure 6.

C - Comparison of Results. A comparison of the results of slow-roll to dynamic and finite element to dynamic stress will now be made. All data that is plotted in the preceding figures were the maximum stress values from the mid-face gage on tooth "B" as shown in Figure 5.

In Figure 10 the effect of the experimental stress measured at slow to moderate speed at light load is made. Figure 10 shows that increasing the speed of the pinion from 1560 to 6000 RPM

had only a very small effect on the stress measured in the range of gear shaft torque from 113 tc 339 N*m (1000 to 3000 in*lb).

In the next comparison, data from the slow roll tests are compared to that taken at two pinion rotational speeds of 11400 and 14400 RPM. This data is shown in Figure 11 for the three pinion rotational speeds and gear shaft torque range of 450 to 1185 N*m (3980 to 10490 in*lb). The data indicates that only a slight increase in stress (less than 10%) was found in going from slow-roll to the highest speed that the tests were conducted.

The last comparison made in this paper is the analytical work with the high-speed dynamic experiments. This comparison is made in Figure 12. The experimental results were attained from the highest stress measured (tooth "B") at the tooth mid-face with the gear shaft torque equal to 1073 N*m (9500 in*lb) at a pinion rotational speed equal to 14400 RPM. The analytical results were taken for the mid-face results from Table 2 for the two teeth monitored. The peek value from the analysis (Tooth 1) was not used in the comparison. For this position in the meshing cycle there was no load sharing due to the model configuration.

The analytical results were oriented to the experimental results with respect to the meshing cycle. From the analysis the results of Table 2 (Reference [15]) showed the stress increasing on Tooth 1 (coming into mesh) and decreasing on Tooth 2 (going out of mesh). The analysis results were oriented to the measured results as a single analytical meshing cycle. When the tooth is carrying substantial load the maximum principal stress plotted agreed fairly well with the experimental results. During the part of the meshing cycle, prior to the tooth carrying load, the finite element results indicated the correct trend but not the correct values. This is caused by the maximum principal stress and the strain gage measurement directions not being oriented in the same direction. An improved assessment of the analytical results in this region (from 250 to 270 degree positions, Figure 12) would be attained by orienting these results in the direction of the strain gage via coordinate transformation.

Obviously a full three-dimensional model including the entire pinion and gear along with support structure would improve the model. However certain compromises need to be made to make the calculations for this highly computer processor intensive analytical approach. Therefore as computers become quicker full simulation modeling will be both practical and inexpensive and model accuracy will be improved.

CONCLUSIONS

From the analytical and experimental results found in this study the following general conclusions can be made:

1. Analytical results predicted the general trend of that found in testing. The deviation of the maximum stress predicted and measured is believed to be due to the model not having the exact attributes (boundary conditions) during the complete meshing cycle.
2. Pinion shaft speed only had a minor effect on the maximum stress found from slow-roll to 14400 RPM. This means that there was little dynamic effect on the stress field.
3. The mid-face location had the highest fillet/root stress followed by the heel location and then the toe location.

REFERENCES

[1] Litvin, F.: Theory of Gearing, NASA RP-1212, AVSCOM TR 90-C-035, Dec. 1989.

[2] Litvin, F.: Gear Geometry and Applied Theory, Prentice Hall, Inc., 1994.

[3] Litvin, F. and Lee, H.: Generation and Tooth Contact Analysis of Spiral Bevel Gears with Predesigned Parabolic Functions of Transmissions Errors, NASA CR-4259, AVSCOM TR 89-C-014, Nov. 1989.

[4] Litvin, F. and Zhang, Y.: Local Synthesis and Tooth Contact Analysis of Face-Milled Spiral Bevel Gears, NASA CR-4342, AVSCOM TR 90-C-028, Jan. 1991.

[5] Stadtfeld, H.: Handbook of Bevel and Hypoid Gears, Rochester Institute of Technology, March 1993.
[6] Krenzer, T.: Tooth Contact Analysis of Spiral Bevel and Hypoid Gears Under Load, SAE Paper 810688, 1981.
[7] Gosselin, C., Cloutier, L. and Brousseau, J.: Tooth Contact Analysis of High Conformity Spiral Bevel Gears, 1991 JSME International Conference on Motion and Power Transmission, Hiroshima, Japan, Nov. 1991.
[8] Wilcox, L. and Coleman, W.: Application of Finite Elements to the Analysis of Gear Tooth Stresses, Journal of Engineering for Industry, Nov. 1973.
[9] Handschuh, R. and Litvin, F.: A Method for Determining Spiral Bevel Gear Tooth Geometry for Finite Element Analysis, NASA TP-3096, AVSCOM TR 91-C-020, Aug. 1991.
[10] Tsai, Y. and Chin, P.: Surface Geometry of Straight and Spiral Bevel Gears, Journal of Mechanical Transmission and Automation in Design, vol. 109, no. 4, Dec. 1987.
[11] Wilcox, L.: An Exact Analytical Method for Calculating Stresses in Bevel and Hypoid Gear Teeth, Int Symp. On Gearing and Power Transmission, Tokyo, Japan, 1981.
[12] Handschuh, R. and Kicher, T.: A Method for Thermal Analysis of Spiral Bevel Gears, Journal of Mechanical Design, Vol. 118, Dec. 1996.
[13] Wilcox, L, and Nowell, G.: Improved Finite Element Model for Calculating Stress in Bevel and Hypoid Gear Teeth, AGMA 97FTM5, Nov. 1997.
[14] Kumar, A. and Bibel, G.: A Procedure for 3-D Contact Stress Analysis of Spiral Bevel Gears, NASA CR-194472, ARL-CR-72, March 1994.
[15] Bibel, G., Tiku, K., and Kumar, A.: Prediction of Contact Path and Load Sharing in Spiral Bevel Gears, NASA CR-195305, ARL-CR-146, April 1994.
[16] Gosselin, C., Gingras, D., Brousseau, J., and Gakwaya, A.:"A Review of the Current Contact Stess and Deformation Formulations Compared to Finite Element Analysis", Proceedings of the 1994 International Gearing Conference, Newcastle, UK.
[17] Bibel, G. and Handschuh, R.: Meshing of a Spiral Bevel Gearset With 3-D Finite Element Analysis, NASA TM-107336, ARL-TR-1224, Oct. 1996.
[18] Albrect, C.: Transmission Design Using Finite Element Analysis Techniques, Proceedings of the Theoretical Basis of Helicopter Technology, Nanjing, PR of China, Nov. 1985.
[19] Henry, Z.: Bell Helicopter Advanced Rotorcraft Transmission (ART) Program, NASA CR-195479, ARL-CR-238, June 1995.
[20] Lewicki, D., Handschuh, R., Henry, Z., and Litvin, F.: Low-Noise, High-Strength, Spiral Bevel Gears for Helicopter Transmission, Journal of Propulsion and Power, vol. 10, no. 3, 1994.
[21] Litvin, F., Wang, A., Handschuh, R., Lewicki, D., and Henry, Z.: Design, Generation, Stress Analysis and Test of Low-Noise, Increased Strength Face-Milled Spiral Bevel Gears, AGMA 97FTM15, Nov. 1997.
[22] PDA Engineering, PATRAN Plus, Release 7.5, Costa Mesa, CA, 1998.
[23] MARC Finite Element Program Revision, K5.2, MARC Analysis Research Corporation, Palo Alto, CA, 1992.
[24] Handschuh, R.:"Effect of Lubricating Jet Location on Spiral Bevel Gear Operatiing Termperatures", NASA TM 105656, AVSCOM Technical Report 91-C-033, September 1992.
[25] Hohn, B.-R., Winter, H., Michaelis, K., and Volhuter, F.: Pitting Resistance and Bending Strength of Bevel and Hypoid Gear Teeth, Proceedings of the 1992 ASME International Power Transmission and Gearing Conference.

Table 1: Design data and machine tool settings for the spiral bevel pinion used in this study.

(a) Pinion design data

Number of teeth (gear ratio)	12 (3.0)
Module, mm (diametral pitch, 1/in.)	4.941 (5.141)
Dedendum angle, deg.	1.5666
Addendum angle, deg.	3.8833
Pitch angle, deg.	18.4333
Shaft angle, deg.	90.0
Mean spiral angle, deg.	35.0
Face width, mm (in.)	25.4 (1.0)
Mean cone distance, mm (in.)	81.05 (3.191)
Inside radius of pinion, mm (in.)	15.5 (0.6094)
Top land thickness, mm (in.)	2.032 (0.080)
Clearance, mm (in.)	0.762 (0.030)

(b) Generation machine settings

	Concave	Convex
Radius of cutter, mm (in.)	75.326 (2.9656)	78.011 (3.0713)
Blade angle, deg.	161.95	24.34
Machine offset, mm (in.)	3.9268 (0.1546)	-4.4262 (-0.1743)
Vector sum, mm (in.)*	0.9779 (0.0385)	-1.3160 (-0.0518)
Cradle to cutter center distance, mm (in.)	74.874 (2.9478)	71.145 (2.8010)
Cradle angle, deg.	63.94	53.96
Ratio of roll	0.30838	0.32204

*Vector sum is equal to the machine center to back setting added vectorally to the sliding base.

Table 2: Fillet stress as a function of rotation angle for different nodes from the element model GPa (ksi).

	Pinion Tooth #1			Pinion Tooth #2		
Node #, Location, axial position along root angle →	A Toe 2.44 mm (0.096 in.)	B Mid-face 13.69 mm (0.535 in.)	C Heel 22.15 mm (0.872 in.)	D Toe 2.44 mm (0.096in.)	E Mid-face 13.69 mm (0.535 in.)	F Heel 22.15 mm (0.872 in.)
Rotation, degrees						
+6	.524 (76.0)	.955 (138)	.226 (32.7)	.270 (39.2)	.128 (18.5)	.105 (15.2)
0	.309 (44.8)	.753 (109)	.262 (38.0)	.313 (45.4)	.111 (16.0)	.089 (12.9)
-6	.166 (24.0)	.459 (66.6)	.202 (29.4)	.464 (67.3)	.123 (17.9)	.075 (10.8)
-12	.071 (10.3)	.149 (21.7)	.086 (12.5)	.513 (74.5)	.199 (28.9)	.066 (9.5)
-18	.026 (3.7)	.009 (1.3)	.041 (5.9)	.565 (82.0)	.384 (55.7)	.080 (11.6)
-24	.003 (0.4)	.110 (16.0)	.091 (13.1)	.623 (90.3)	.469 (68.0)	.101 (14.6)
-30	.013 (1.8)	.203 (29.5)	.116 (16.8)	.261 (37.9)	.559 (81.1)	.188 (27.3)

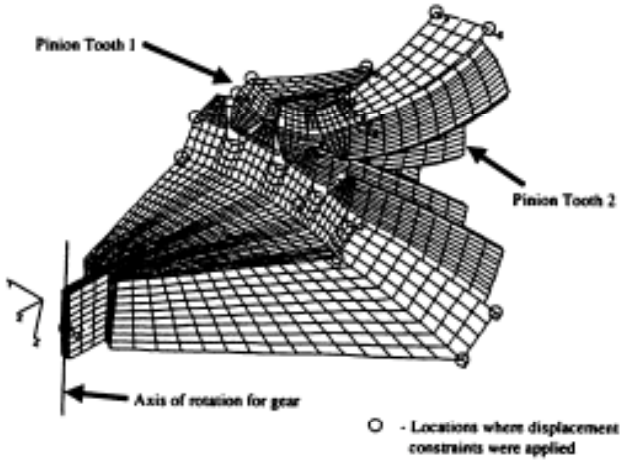

Figure 1: Seven-tooth model used in finite element analysis.

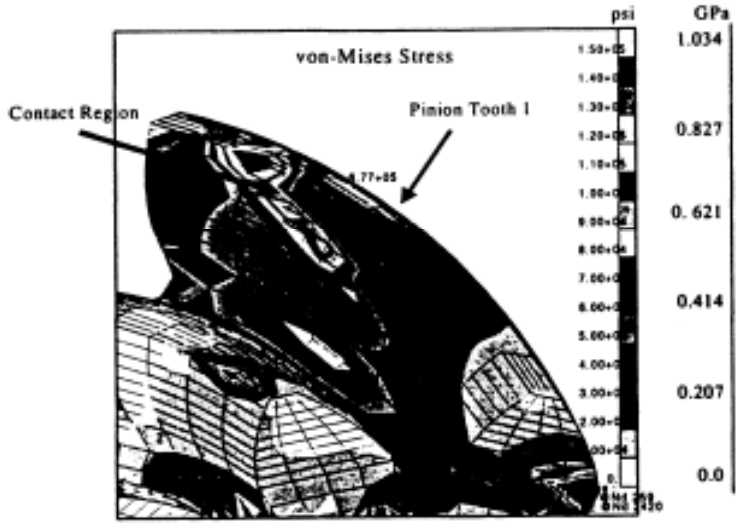

Figure 2: Example of finite element results from 3-D contact analysis at gear torque equal to 1073 N*m (9500 in*lb).

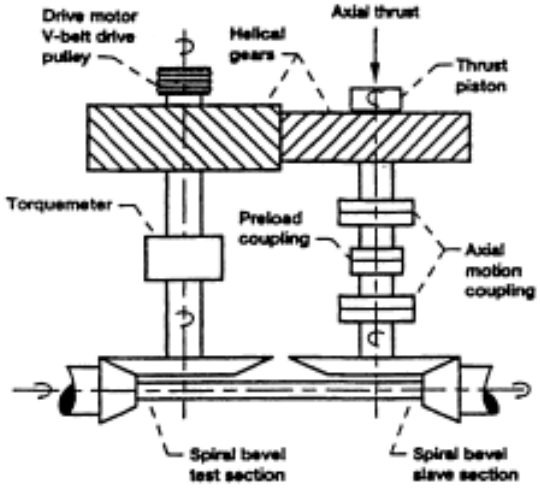

Figure 3: Cross-sectional view of spiral bevel gear test facility.

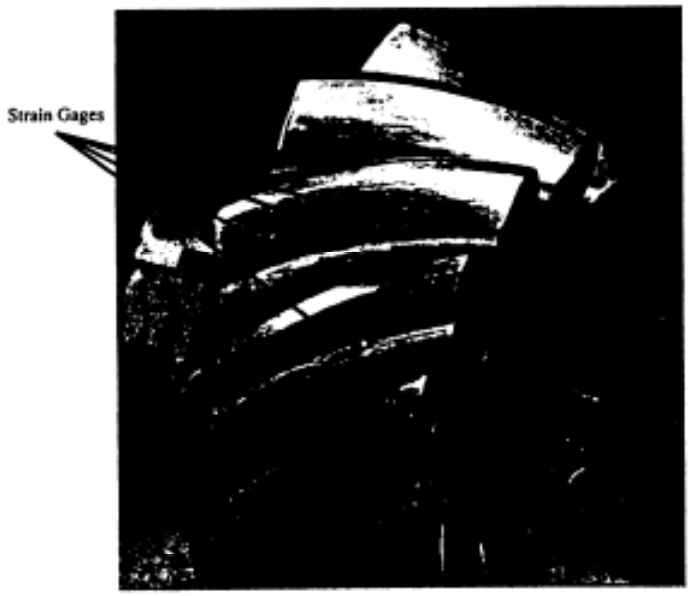

Figure 4: Instrumented pinion used in experiments.

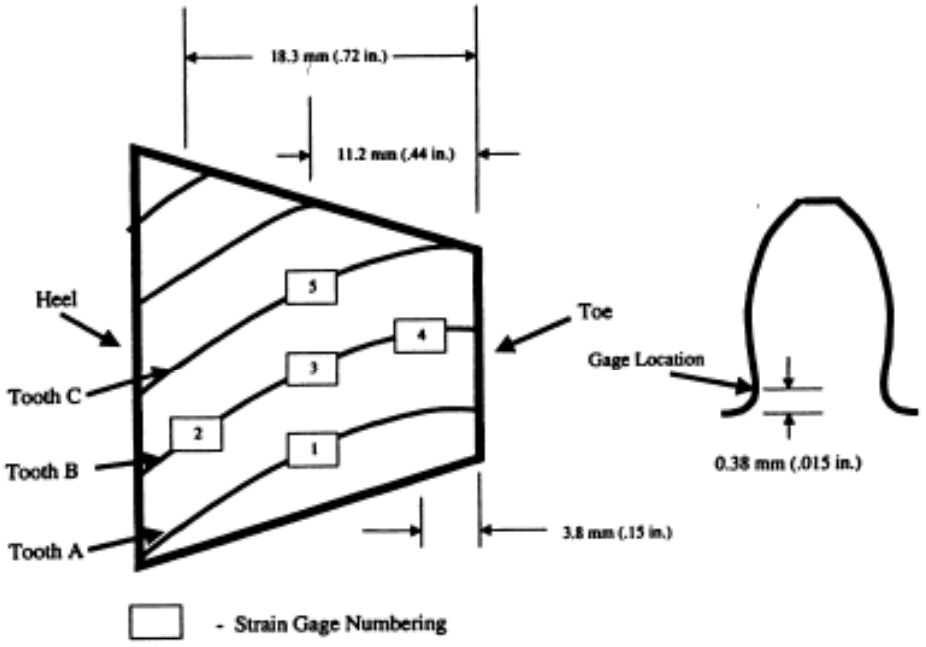

Figure 5: Strain gage location on the three successive teeth (position along root angle from toe of pinion).

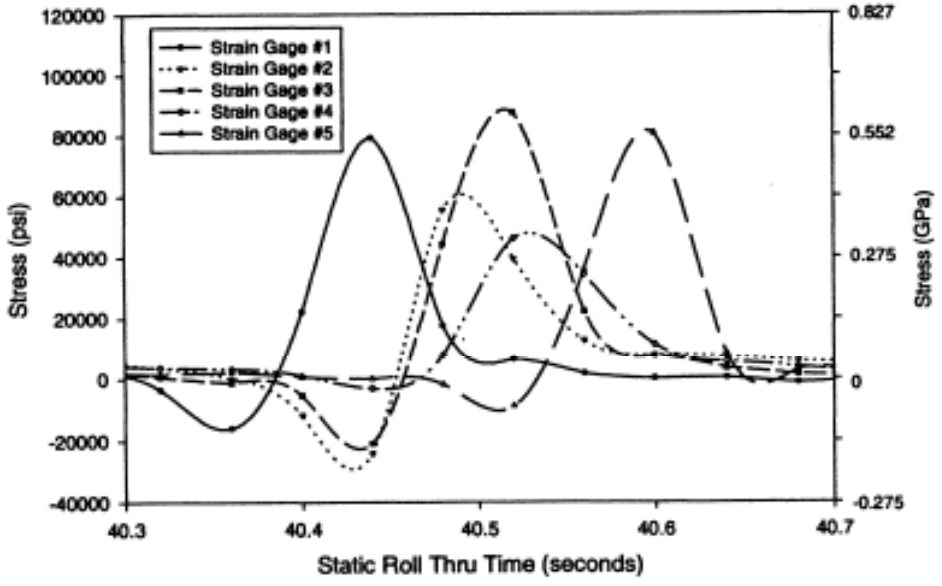

Figure 6: Slow roll through mesh data at 885.8 N*m (7840 in*lb) gear shaft torque.

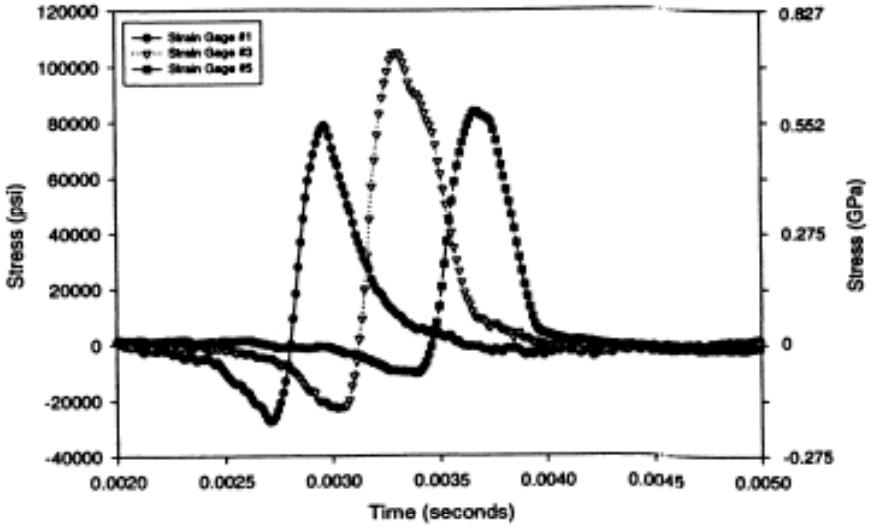

Figure 7: Dynamic data taken at pinion shaft speed of 14400 RPM, and gear shaft torque equal to 1073 N*m (9500 in*lb).

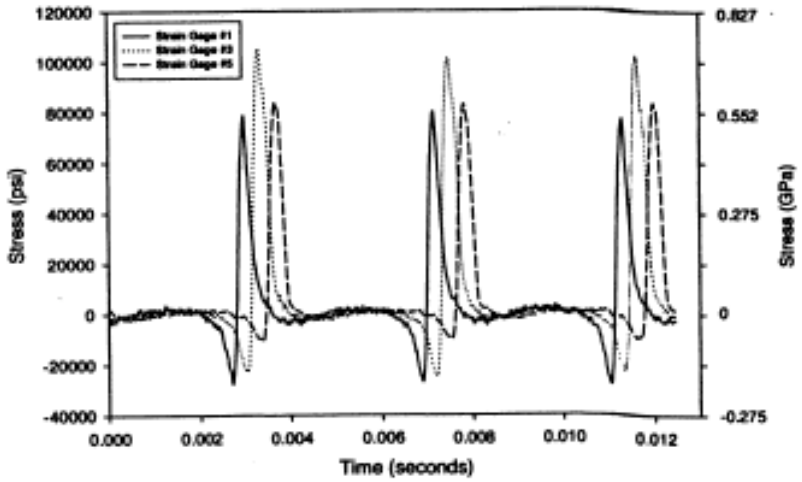

Figure 8: Dynamic data for the same conditions as Figure 7 but for three pinion revolutions.

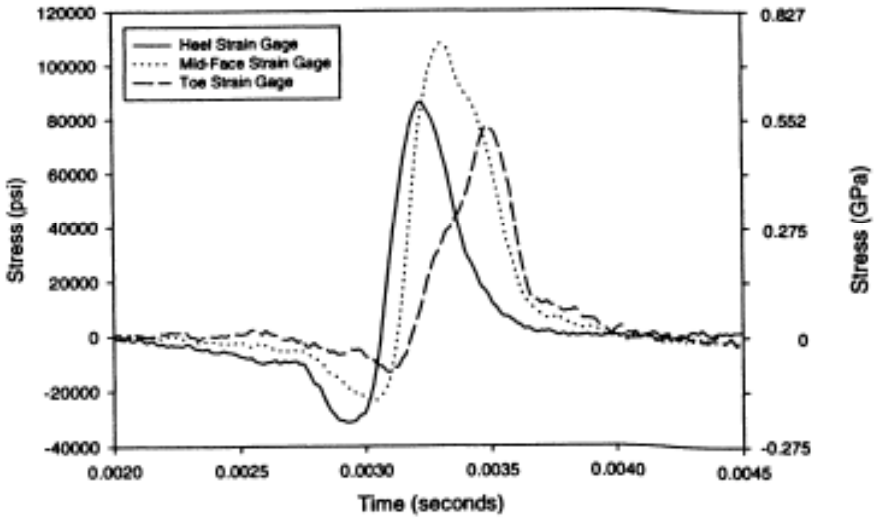

Figure 9: Dynamic data taken at pinion rotational speed of 14400 RPM and gear shaft torque equal to 1073 N*m (9500 in*lb) showing the results from all three strain gages on a single tooth.

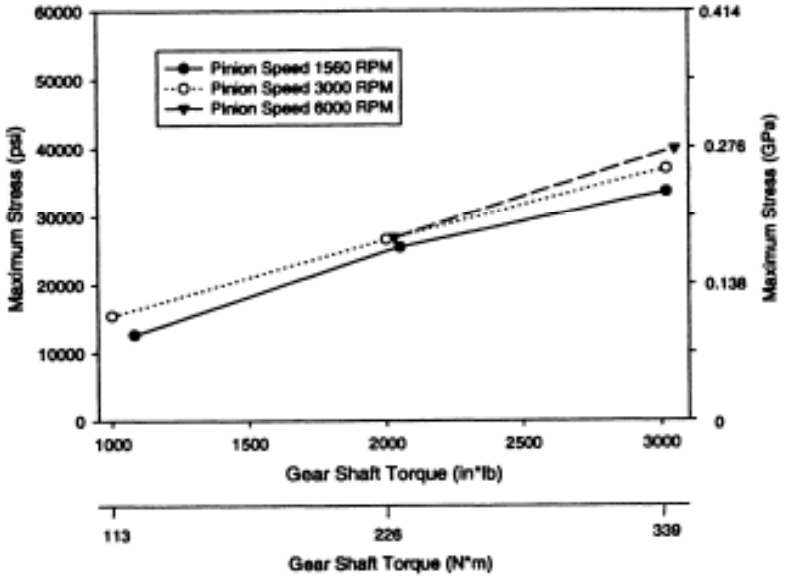

Figure 10: Effect of speed on measured maximum stress.

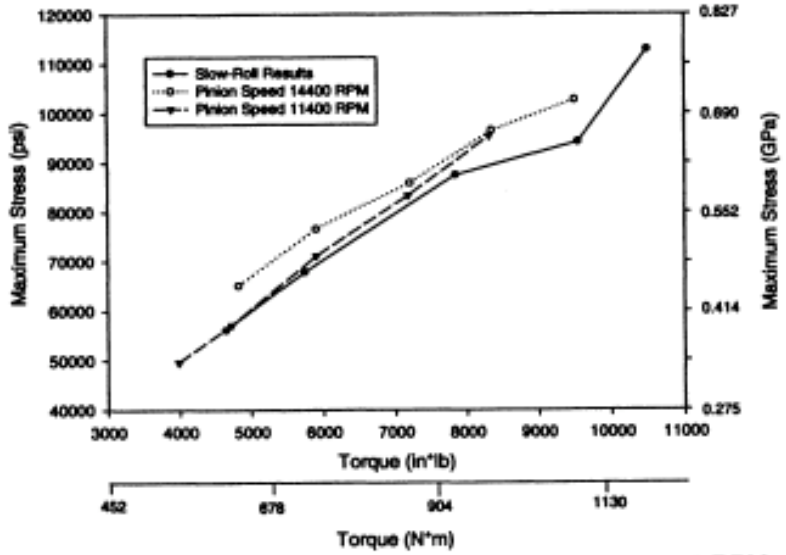

Figure 11: Comparison of slow roll data to that taken at 14400 RPM. Applied torque was measured at the gear shaft.

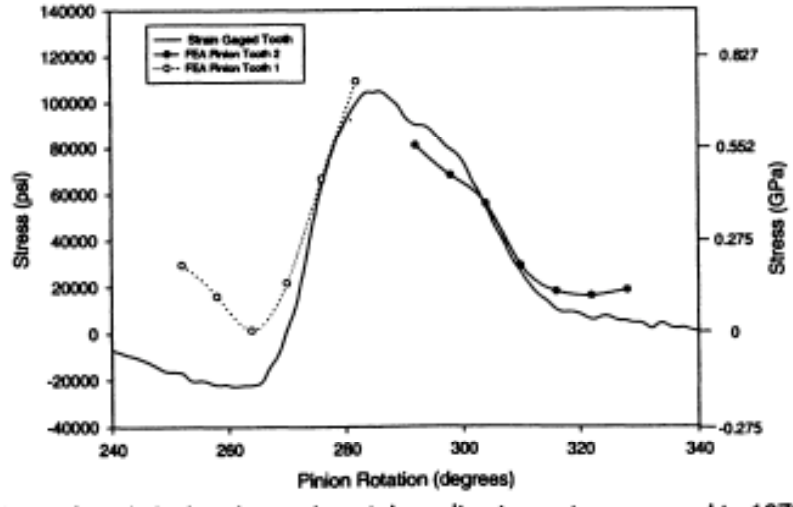

Figure 12: Comparison of analytical and experimental results at gear torque equal to 1073 N*m (9500 in*lb).